Supporting Information

Thermal Transport Driven by Extraneous Nanoparticles and Phase Segregation in Nanostructured $Mg_2(Si,Sn)$ and Estimation of Optimum Thermoelectric Performance

Abdullah S. Tazebay[1], Su-In Yi[1], Jae Ki Lee[2], Hyunghoon Kim[3], Je-Hyeong Bahk[4], Suk Lae Kim[1], Su-Dong Park[2], Ho Seong Lee[3], Ali Shakouri[4], Choongho Yu[1,*]

[1]Department of Mechanical Engineering, Texas A&M University, College Station, TX 77843, USA

[2]Korea Electrotechnology Research Institute, Changwon, Korea

[3]School of Materials Science and Engineering, Kyungpook National University, 80 Daehak-ro, Buk-gu, Daegu 702-701, Korea

[4]Birck Nanotechnology Center, Purdue University, West Lafayette, IN 47907, USA

*Corresponding author: chyu@tamu.edu

Table S1. Atomic ratios of raw elements and volume fractions of TiO_2 nanoparticles in 12 different kinds of solid solutions made of magnesium silicide and magnesium stannide. Note that 10% excessive magnesium was used to compensate loss during synthesis processes.

<table>
<tr><th rowspan="2">Sample no.</th><th>Volume fraction</th><th colspan="5">Atomic ratio</th></tr>
<tr><th>TiO_2</th><th>Sn</th><th>Sb</th><th>Si</th><th>As</th><th>Mg</th></tr>
<tr><td>1</td><td>0%</td><td rowspan="4">0.5925</td><td rowspan="4">0.0075</td><td rowspan="12">0.392</td><td rowspan="12">0.008</td><td rowspan="12">2.2</td></tr>
<tr><td>2</td><td>1%</td></tr>
<tr><td>3</td><td>2%</td></tr>
<tr><td>4</td><td>5%</td></tr>
<tr><td>5</td><td>0%</td><td rowspan="8">0.585</td><td rowspan="8">0.015</td></tr>
<tr><td>6</td><td>0.1%</td></tr>
<tr><td>7</td><td>0.2%</td></tr>
<tr><td>8</td><td>0.5%</td></tr>
<tr><td>9</td><td>1%</td></tr>
<tr><td>10</td><td>2%</td></tr>
<tr><td>11</td><td>5%</td></tr>
<tr><td>12</td><td>10%</td></tr>
</table>

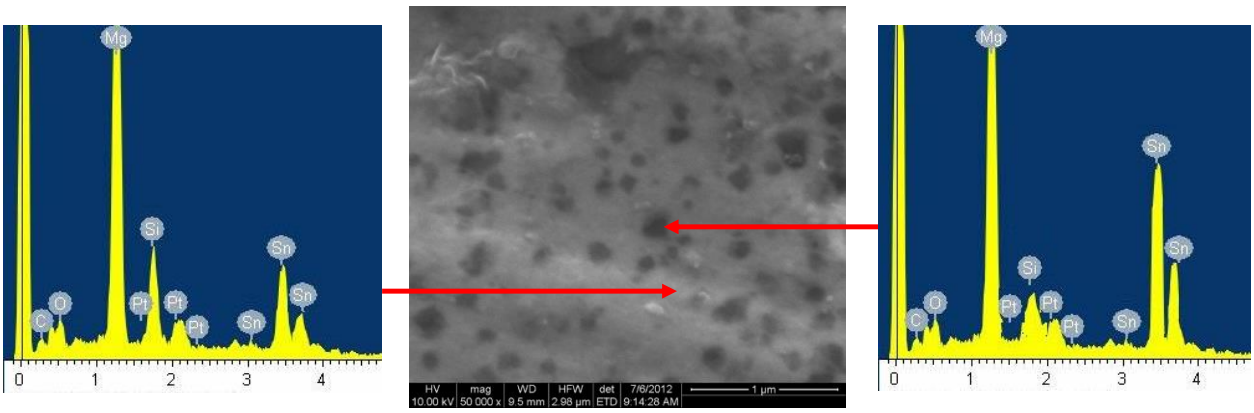

Figure S1. Scanning electron microscope (SEM) image with energy dispersive spectroscopy (EDS) results on dark and grey regions.

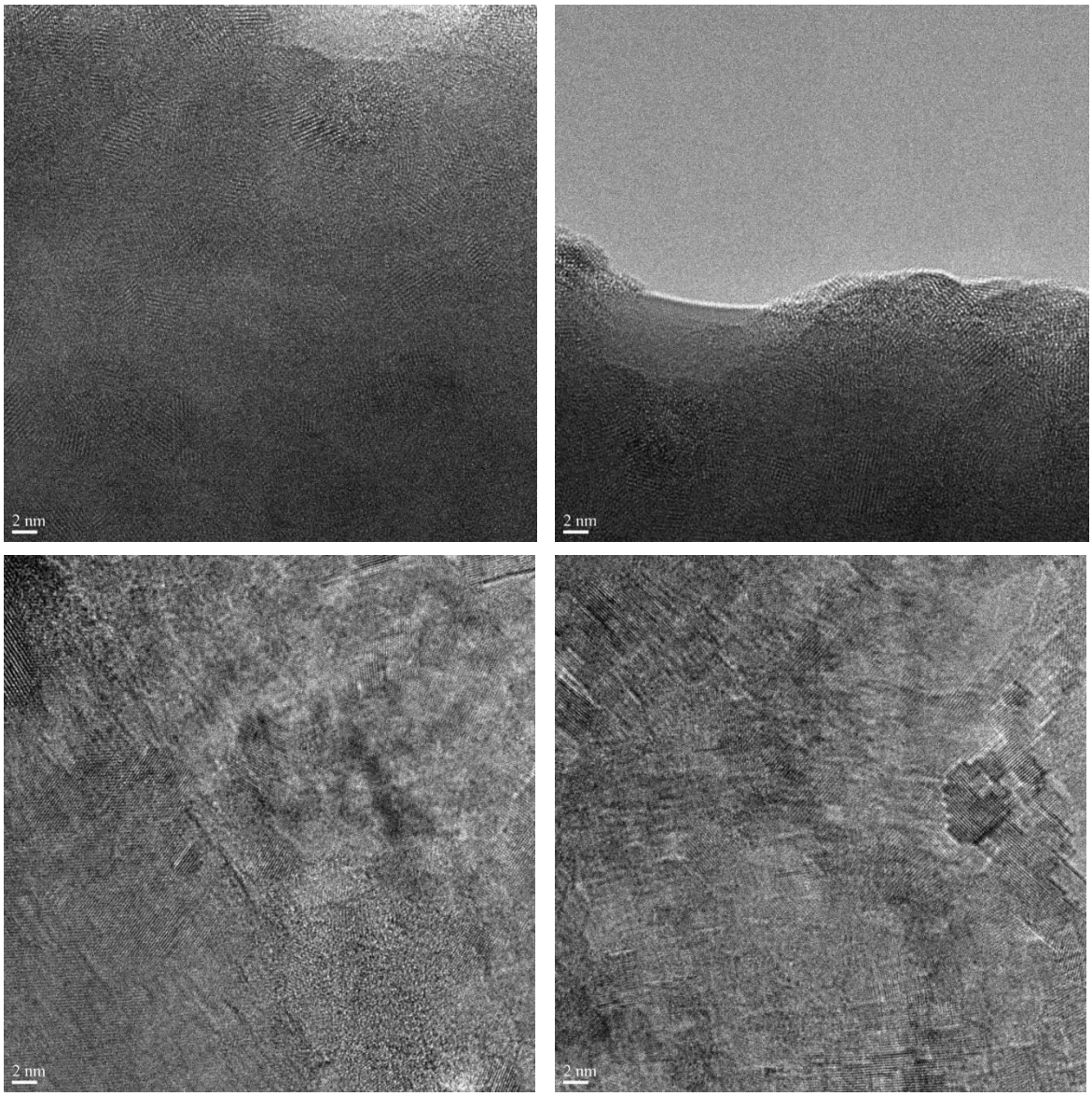

Figure S2. High resolution transmission electron microscope (TEM) images used to determine distribution of nanograin sizes. The scale bar indicates 2 nm (continued to the next page).

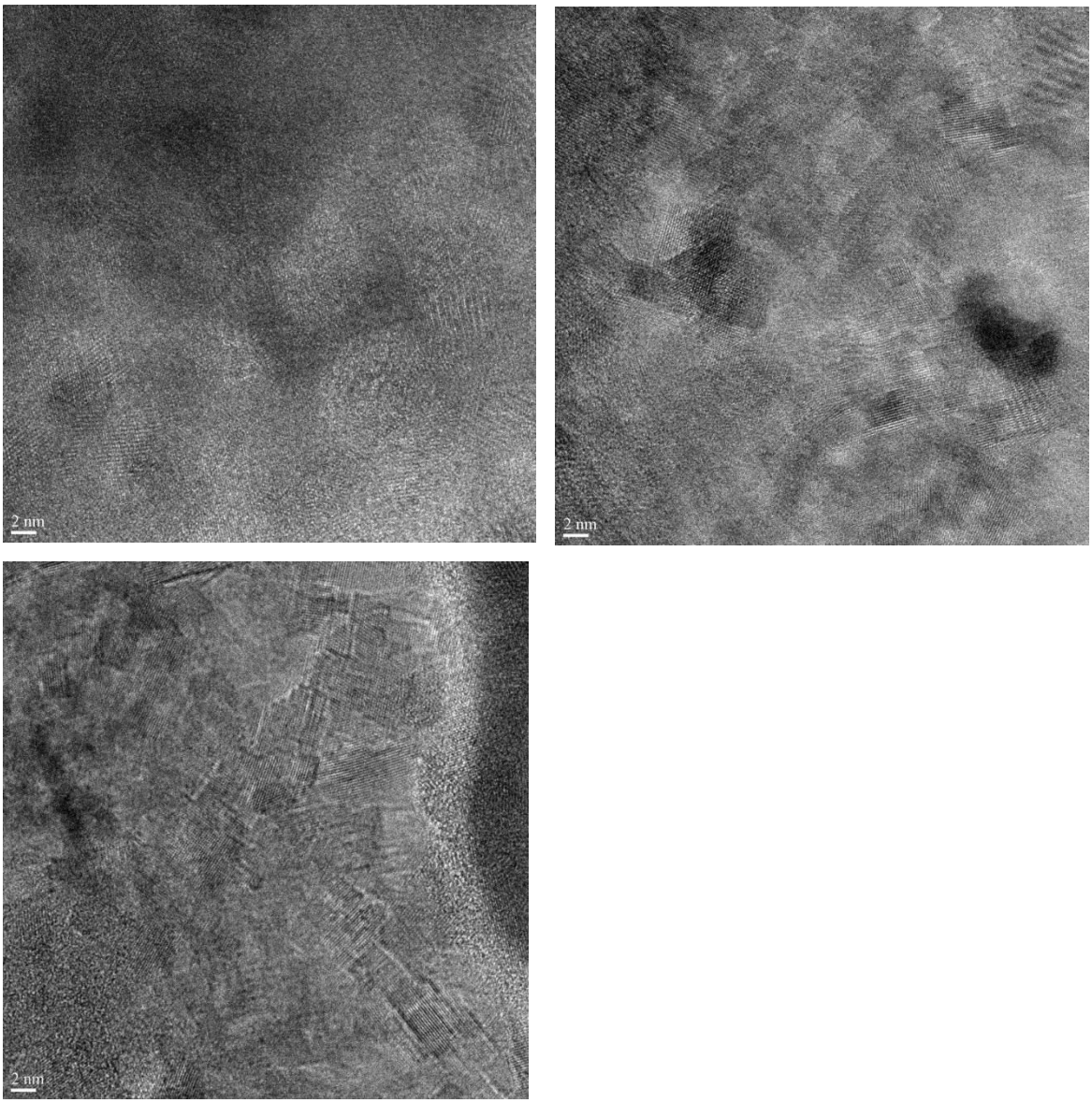

Figure S2. (continued from the previous page)

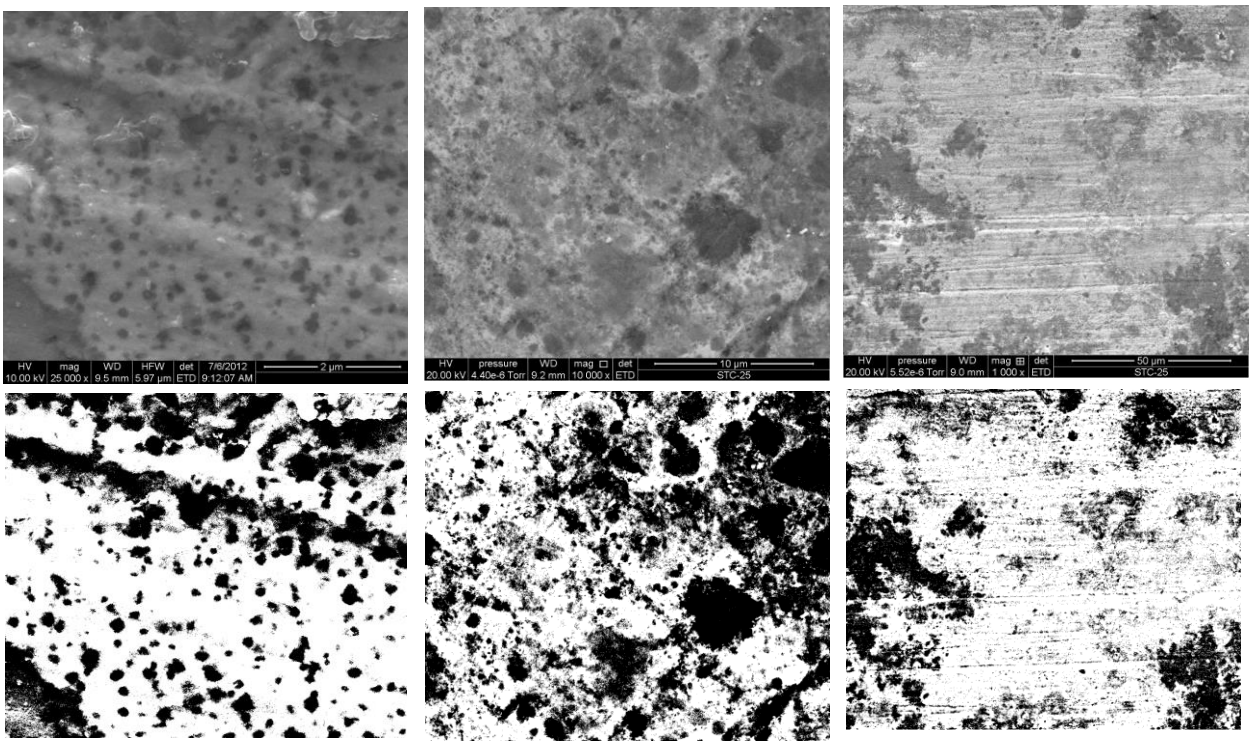

Figure S3. SEM images (upper row) used to estimate the ratio of phase segregation percentage and binary masks (lower row) created from those figures in the first row by using ImageJ.

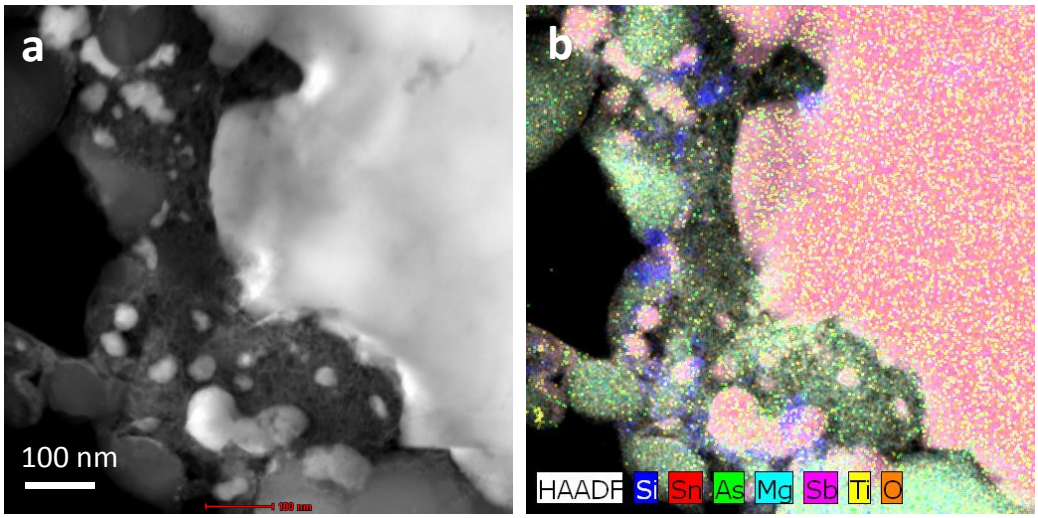

Figure S4. (a) TEM-EDS elemental mapping of Sample 6 (2% TiO_2). (b) Colored mapping results of Si, Sn, As, Mg, Sb, Ti, and O.

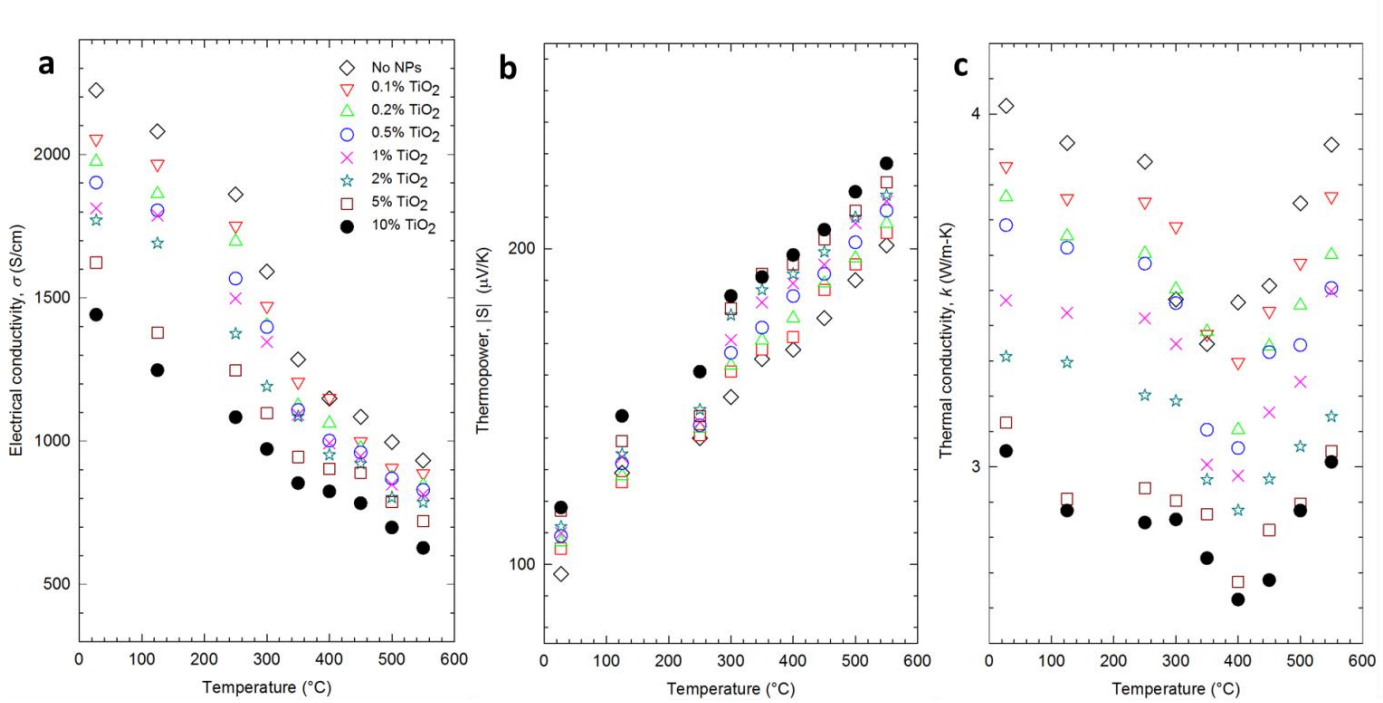

Figure S5. Electrical conductivity (a), thermopower (b), and thermal conductivity (c) of Sample 5~12 containing TiO_2 nanoparticles (0~10 vol%) and 1.5% Sb dopants.

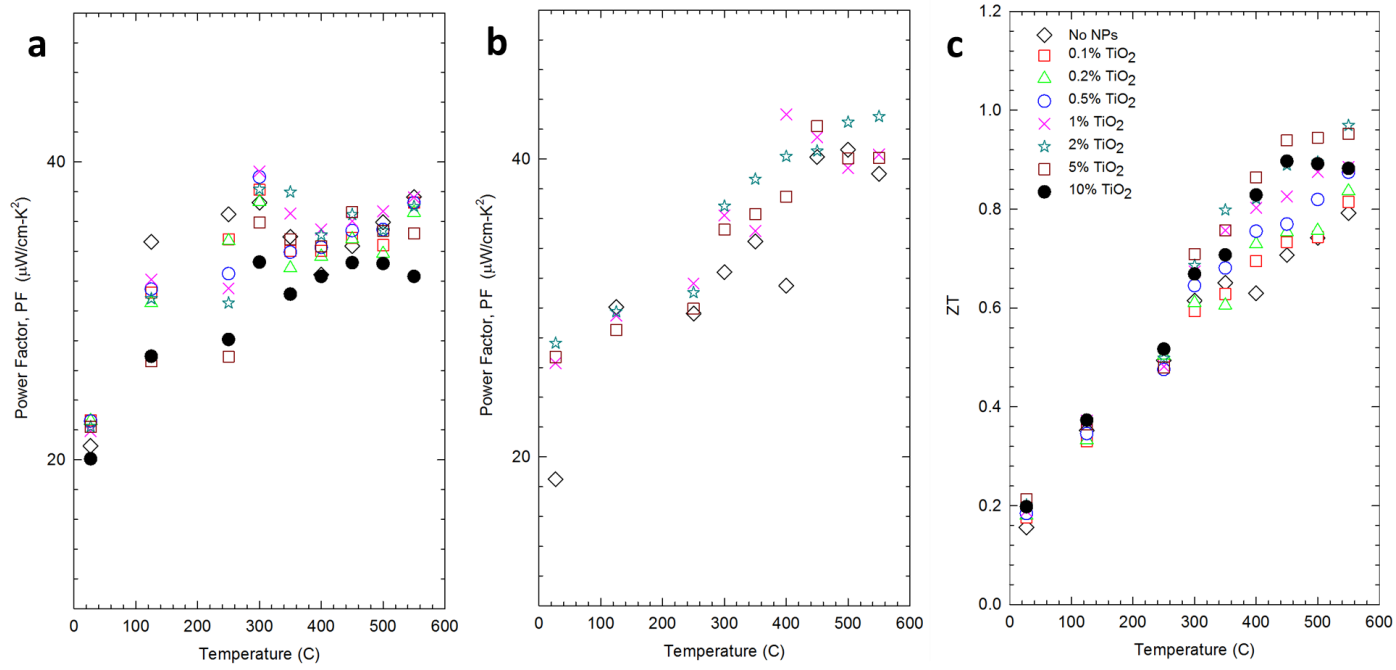

Figure S6. Thermoelectric power factor of Sample 5~12 (a) and Sample 1~4 (b). Thermoelectric figure of merit (*ZT*) of Sample 5~12 (c).

Electrical Conductivity and Thermopower Calculation

Electron (or majority) carrier concentration (N_e) and hole (or minority) carrier concentration (N_h) can be calculated with the Fermi levels as input parameters:

$$N_e = N_{V,X3}\int_0^\infty \frac{\sqrt{2E}\left(m^*_{X3}\right)^{1.5}/\left(\pi^2\hbar^3\right)}{\exp\left[\left(E-E_{F,X3}\right)/\left(k_BT\right)\right]+1}dE + N_{V,X1}\int_0^\infty \frac{\sqrt{2E}\left(m^*_{X1}\right)^{1.5}/\left(\pi^2\hbar^3\right)}{\exp\left[\left(E-E_{F,X1}\right)/\left(k_BT\right)\right]+1}dE \quad \text{(S1)}$$

$$N_h = N_{V,HH}\int_0^\infty \frac{\sqrt{2E}\left(m^*_{HH}\right)^{1.5}/\left(\pi^2\hbar^3\right)}{\exp\left[\left(E-E_{F,HH}\right)/\left(k_BT\right)\right]+1}dE + N_{V,LH}\int_0^\infty \frac{\sqrt{2E}\left(m^*_{LH}\right)^{1.5}/\left(\pi^2\hbar^3\right)}{\exp\left[\left(E-E_{F,LH}\right)/\left(k_BT\right)\right]+1}dE \quad \text{(S2)}$$

Here we considered two X-valleys in the conduction band (labeled as X1 and X3) and two Γ-valleys in the valence band (labeled as HH, and LH), as shown in Fig. S6.[1] Each integral was calculated with respect to the band edge of each valley (*i.e.*, $E = 0$ at the band edge). For convenience, we used the band edge of X3 valley as a reference, the four valleys can be expressed with the Fermi level (E_F) as:

$$E_{F,X3} = E_F \quad \text{(S3)}$$

$$E_{F,X1} = E_F - E_0 \quad \text{(S4)}$$

$$E_{F,HH} = E_{F,LH} = -\left(E_G + E_F\right) \quad \text{(S5)}$$

where E_0 is the energy offset ($E_{Edge,X1} - E_{Edge,X3}$) and E_G is the band gap as shown in Fig. S6.

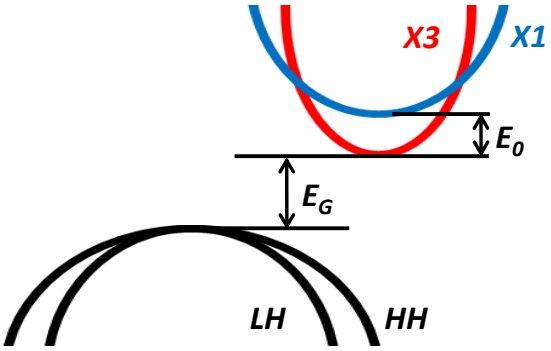

Figure S7. Multi valley schematic of $Mg_2Si_{0.4}Sn_{0.6}$.

With the effective mass (m^*) in Table S1, N_e and N_h were found, and then ionized impurity concentration (N_{II}) was calculated by:

$$N_{II} = N_e - N_h \quad \text{(S6)}$$

Thermopower (S) can be calculated with electrical conductivity (σ) by:

$$S = \sum_j S_j \frac{\sigma_j}{\sigma} \tag{S7}$$

$$S_j = \int_0^\infty \frac{\sigma_{d,j}(E)}{\sigma_j}\left(\frac{E - E_{F,j}}{qT}\right)dE \tag{S8}$$

$$\sigma_{d,j}(E) = q^2 \times D_j(E) \times \left(-\frac{df_j(E)}{dE}\right) \times \tau_j(E) \times \left\{v_j(E)\right\}^2 \tag{S9}$$

$$D_j(E) = \frac{\sqrt{2}(m_j^*)^{1.5}}{\pi^2\hbar^3}\sqrt{E} \tag{S10}$$

$$f_j(E) = \frac{1}{\exp\left[\left(E - E_{F,j}\right)/\left(k_B T\right)\right] + 1} \tag{S11}$$

$$\tau_j(E) = \left(\tau_{AC,j}^{-1}(E) + \tau_{II,j}^{-1}(E) + \tau_{POP,j}^{-1}(E) + \tau_{NI,j}^{-1}(E)\right)^{-1} \tag{S12}$$

$$v_j(E) = \sqrt{\frac{2E}{3m_j^*}} \tag{S13}$$

$$\sigma_j = N_{V,j}\int_0^\infty \sigma_{d,j}(E)dE \tag{S14}$$

$$\sigma = \sum_j \sigma_j \tag{S15}$$

where q, T, E, m^*, N_V are electron charge, absolute temperature, carrier energy with respect to band edge, carrier effective mass, and valley degeneracy, respectively. The index j indicates valley (X1, X3, HH, and LH). The subscripts AC, POP, II, and NI in scattering relaxation time represent acoustic phonon, ionized impurity, polar optical phonon, non-ionized impurity, respectively. The material parameters employed are summarized in Table S2.

The mobility of electron (μ_e) and hole (μ_h) carriers can be obtained by:

$$\mu_e = \frac{\sigma_{X1} + \sigma_{X3}}{qN_e} \tag{S16}$$

$$\mu_h = \frac{\sigma_{HH} + \sigma_{LH}}{qN_h} \tag{S17}$$

The mean free path of electronic carrier (l_j) as a function of energy in valley j can be obtained by:

$$l_j = \sqrt{\frac{2E}{m_j^*}} \times \tau_j \tag{S18}$$

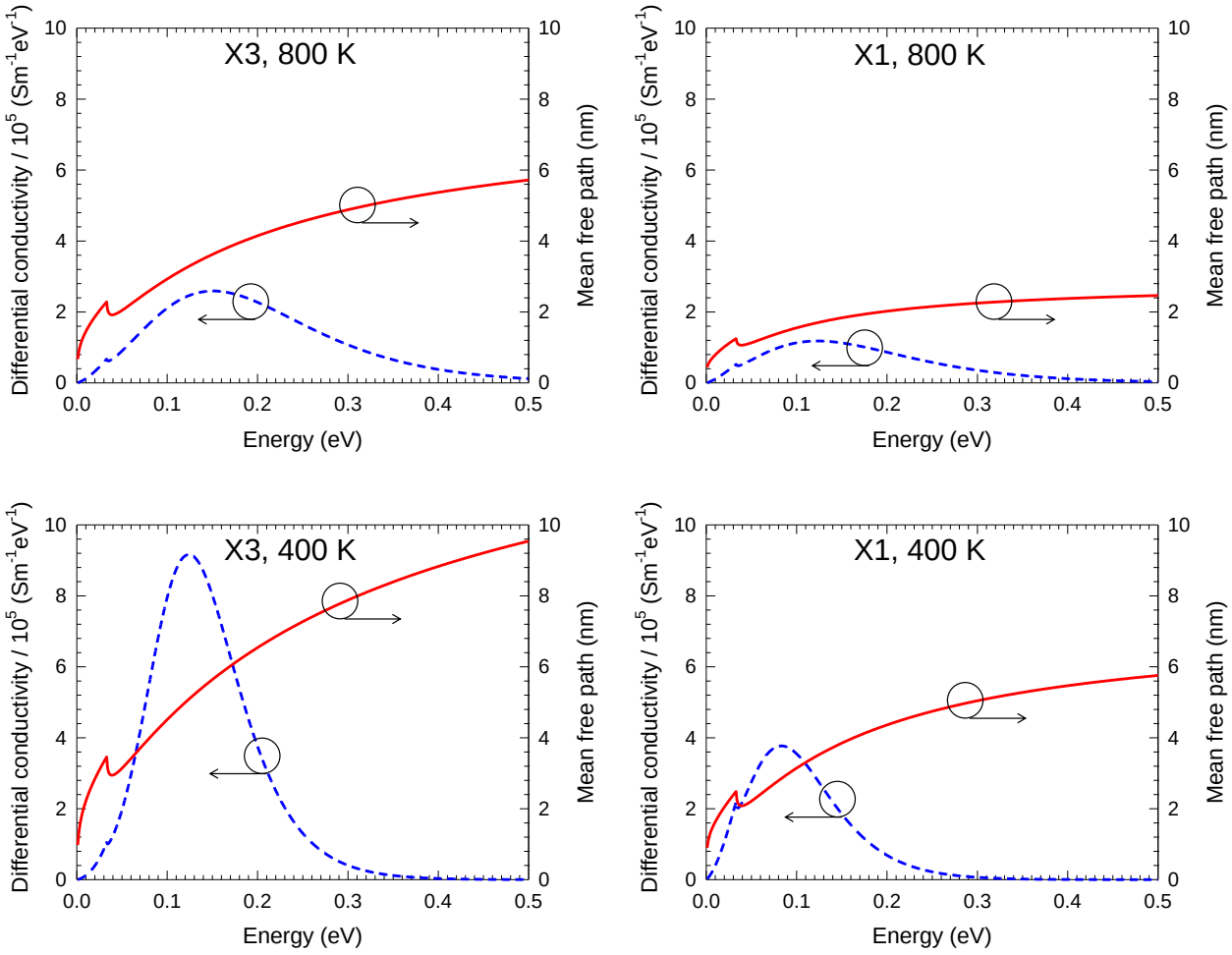

Figure S8. Calculated mean free path of electron carriers in X3 and X1 valley as a function of energy for no TiO_2 nanoparticle sample at 800 K and 400 K using the velocity and relaxation time.

Table S2. Parameters used for calculation.[1-2] The atomic concentration of Sn is y.

Parameters	Values
m^*_{X3} (m_0)	0.38
m^*_{X1} (m_0)	$0.49+2.0\times10^{-4}\times T$
m^*_{HH} (m_0)	1.5
m^*_{LH} (m_0)	1.0
E_G (eV)	$(0.78-4.0\times10^{-4}\times T)\times(1-y) + (0.38-2.8\times10^{-4}\times T)\times y$
E_0 (eV)	$(0.4)\times(1-y) + (-0.165)\times y$
ε_0 (F/m)	$(20\times(1-y) + 23.75\times y)\times8.85\times10^{-12}$
ε_∞ (F/m)	$(13.3\times(1-y) + 17\times y)\times8.85\times10^{-12}$
$\hbar\omega_0$ (meV)	$40\times(1-y)+28.8\times y$
ρ_{NP} (g/cm^3)	3.78
d (nm)	11
ρ_M (g/cm^3)	$1.88\times(1-y)+3.59\times y$
D_e (eV)	7
D_h (eV)	1
C_l (N/m^2)	$(4.15\times(1-y)+3.22\times y)\times10^{10}$
$\omega_{C,L}$ (THz)	$52.3\times(1-y)+ 22.4\times y$
$\omega_{C,T}$ (THz)	$29.7\times(1-y)+ 13.9\times y$
v_L (m/s)	$7700\times(1-y)+ 4900\times y$
v_T (m/s)	$4900\times(1-y)+ 3000\times y$
γ	$2.5\times(1-y)+ 1.7\times y$
α for TiO_2 0%, 1%, 2%, 5%	Respectively 0.65, 0.60, 0.55, 0.50
β for TiO_2 0%, 1%, 2%, 5%	Respectively 1, 0.8, 0.6, 0.5
$N_{V,X3}$, $N_{V,X1}$	3
$N_{V,HH}$, $N_{V,LH}$	1

Thermal Conductivity Calculation

Electronic thermal conductivity (k_e) and bipolar thermal conductivity (k_{bi}) can be calculated by:

$$k_e = \sum_j L_j \sigma_j T \tag{S19}$$

The Lorenz number is expressed as:

$$L_j = \int_0^\infty \frac{\sigma_{d,j}(E)}{\sigma_j}\left(\frac{E - E_{F,j}}{qT}\right)^2 dE - \left\{\int_0^\infty \frac{\sigma_{d,j}(E)}{\sigma_j}\left(\frac{E - E_{F,j}}{qT}\right)dE\right\}^2 \tag{S20}$$

$$k_{bi} = \frac{\sigma_e \sigma_h}{\sigma_e + \sigma_h}(S_e - S_h)^2 T \tag{S21}$$

where

$$\sigma_e = \sigma_{X1} + \sigma_{X3};\ \ \sigma_h = \sigma_{HH} + \sigma_{LH} \tag{S22}$$

$$S_e = \frac{\sigma_{X1}S_{X1} + \sigma_{X3}S_{X3}}{\sigma_e};\ S_h = \frac{\sigma_{HH}S_{HH} + \sigma_{LH}S_{LH}}{\sigma_h} \tag{S23}$$

Lattice thermal conductivity was calculated by using a modified Callaway model that separately considered longitudinal and transverse modes of phonons.

$$k_l = \frac{1}{3}(k_L + 2k_T) \tag{S24}$$

$$k_i = \frac{k_B^4 T^3}{2\pi^2 \hbar^3}\left(\frac{1}{v_i}\right)\left(I_{i1} + \frac{I_{i2}^{\ 2}}{I_{i3}}\right) \tag{S25}$$

The subscript i stands for either longitudinal mode (L) or transverse mode (T).

$$I_{i1} = \int_0^{\theta_i/T} \tau_{p,i} \frac{x^4 e^x}{(e^x - 1)^2} dx \tag{S26}$$

$$I_{i2} = \int_0^{\theta_i/T} \frac{\tau_{p,i}}{\tau_{pN,i}} \frac{x^4 e^x}{(e^x - 1)^2} dx \tag{S27}$$

$$I_{i3} = \int_0^{\theta_i/T} \frac{\tau_{p,i}}{\tau_{pN,i}\tau_{pR,i}} \frac{x^4 e^x}{(e^x - 1)^2} dx \tag{S28}$$

where $x=\hbar\omega/(k_B T)$ is the reduced energy of phonon and Θ_i is the Debye temperature.

$$\frac{1}{\tau_{p,i}} = \frac{1}{\tau_{pN,i}} + \frac{1}{\tau_{pR,i}} \tag{S29}$$

The relaxation time corresponding to the normal scattering is described as:[3]

$$(\tau_{pN,L})^{-1} = \frac{k_B^5 \gamma^2 V}{M v_L^5 \hbar^4} x^2 T^5 \tag{S30}$$

$$(\tau_{pN,T})^{-1} = \frac{k_B^5 \gamma^2 V}{M v_T^5 \hbar^4} x T^5 \tag{S31}$$

where k_B, γ, V, M, v_L, v_T, $\hbar$ and T are Boltzmann constant, Grüneisen parameter, average volume of an atom, average mass of an atom, longitudinal sound velocity, transverse sound velocity, reduced Planck constant, and absolute temperature, respectively.

Umklapp scattering is expressed as:

$$(\tau_{pU,i})^{-1} = \frac{\hbar \gamma^2}{M v_i^2 \theta_i} \left(\frac{k_B}{\hbar} \right)^2 x^2 T^3 e^{-\theta_i / 3T} \tag{S32}$$

where θ_i is the Debye temperature which is equal to $\hbar\omega_C/k_B$. The scattering due to random alloy between Si and Sn is

$$(\tau_{pA,i})^{-1} = \Gamma \frac{V}{4\pi v_i^3} \left(\frac{k_B T}{\hbar} \right)^4 x^4 \tag{S33}$$

$$\Gamma = 3 \left(\frac{M_{Si,Sn}}{2M_{Mg} + M_{Si,Sn}} \right)^2 \left((1-y) \left(\frac{M_{Si} - M_{Si,Sn}}{M_{Si,Sn}} \right)^2 + y \left(\frac{M_{Sn} - M_{Si,Sn}}{M_{Si,Sn}} \right)^2 \right) \tag{S34}$$

$$M_{Si,Sn} = (1-y) M_{Si} + y M_{Sn} \tag{S35}$$

where y is the atomic ratio of Sn, which is 0.6 for $Mg_2Si_{0.4}Sn_{0.6}$, and $M_{Si,Sn}$ is the average atomic mass of Si and Sn accordingly with the ratio y.

Phonon scattering by electronic carriers was considered by using:

$$(\tau_{pE,i})^{-1} = (\tau_{pE,i,X3})^{-1} + (\tau_{pE,i,X1})^{-1} \tag{S36}$$

$$(\tau_{pE,i,j})^{-1} = N_{V,j} \frac{D_e^2 (m_j^*)^3 v_i}{4\pi\hbar^4 \rho \beta_{i,j}} \left\{ x - \ln \left[\frac{1 + e^{(\beta_{i,j} - \frac{E_{F,j}}{k_B T} + x^2/(16\beta_{i,j}) + x/2)}}{1 + e^{(\beta_{i,j} - \frac{E_{F,j}}{k_B T} + x^2/(16\beta_{i,j}) - x/2)}} \right] \right\} \tag{S37}$$

$$\beta_{i,j} = \frac{m_j^* v_i^2}{2k_B T} \tag{S38}$$

where D_e and ρ are electron deformation potential and density of $Mg_2Si_{0.4}Sn_{0.6}$, respectively. We ignored phonon scattering due to holes (minority carriers) since its influence on the total relaxation time is very small.

Phonon scattering by nanoparticles was considered by using:

$$(\tau_{pNP,i})^{-1} = \varsigma \frac{\pi v_i N_{NP} D_{NP}^6 k_B^4 x^4 T^4}{2k_B^4 D_{NP}^4 x^4 T^4 + 32\hbar^4 v_i^4} \tag{S39}$$

$$\varsigma = 1 - \exp\left(-\frac{\rho_{NP} - \rho_M}{\rho_M} \right) \tag{S40}$$

where N_{NP} is the concentration of nanoparticles and D_{NP} is the diameter of nanoparticles with the assumption of a sphere shape. λ accounts for the density difference between the matrix material and TiO_2 nanoparticles. λ approaches 1 when the density difference is infinity. N_{NP} and D_{NP} are related each other since the volume percent of TiO_2 nanoparticles is given.

$$N_{NP} = \frac{X/100}{\frac{4\pi}{3}\left(\frac{D_{NP}}{2}\right)^3} \tag{S41}$$

where X is the volume percent of TiO_2. N_{NP} was found to be 1.5×10^{17}, 3.1×10^{17}, and 2.8×10^{16} cm^{-3} respectively for samples with 1%, 2%, and 5% TiO2 nanoparticles.

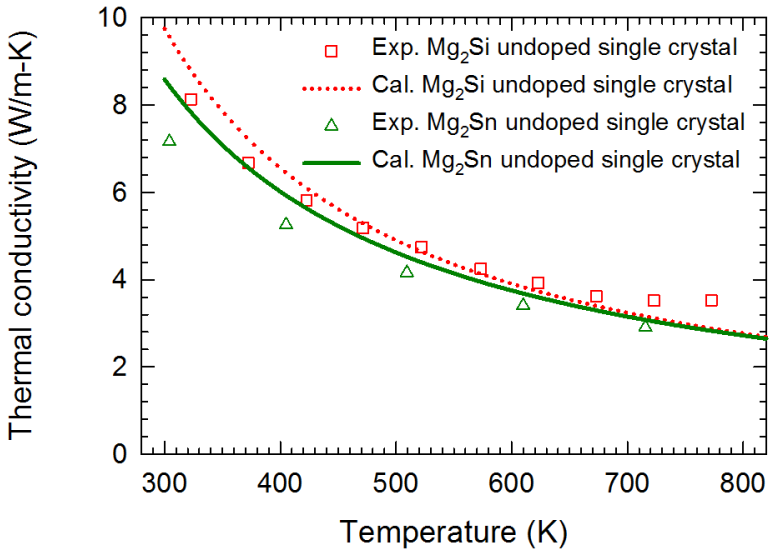

Figure S9. Undoped single crystalline Mg_2Si and Mg_2Sn data[4-5] was fitted to find the Grüneisen parameters (2.5 and 1.7) by considering normal scattering and Umklapp scattering.

Phase segregation was calculated by using the area percentage of Mg_2Sn (A_{Mg2Sn}) obtained from ImageJ software.[6] The segregated Mg_2Si (A_{Mg2Si}) phase was calculated by multiplying A_{Mg2Sn} and both atomic ratio (0.6:0.4 for Sn:Si) and areal ratio (square of lattice constant).

$$A_{Mg_2Si} = A_{Mg_2Sn}\left(\frac{a^2_{Mg_2Si}}{a^2_{Mg_2Sn}} \times \frac{0.6}{0.4}\right) \tag{S42}$$

where a_{Mg2Si} and a_{Mg2Sn} are lattice constants of Mg_2Si and Mg_2Sn, respectively. The total segregated portion was obtained by adding the two segregated areas.

$$A_{Total} = A_{Mg_2Si} + A_{Mg_2Sn} \tag{S43}$$

It should be noted that the areal ratio for the two phases is the same as the volumetric ratio, assuming that

the thickness is the same for both.

The relaxation time of holes (minority carriers) was adjusted with a multiplying factor β, ranging from 0 to 1 in order to consider the reduction of bipolar thermal conductivity due to the minority carrier scattering by TiO_2 nanoparticles. For the sample without TiO_2 nanoparticles, β=1.

$$\tau_{HH}(E) = \beta\left(\tau_{AC,HH}^{-1}(E) + \tau_{II,HH}^{-1}(E) + \tau_{POP,HH}^{-1}(E) + \tau_{NI,HH}^{-1}(E)\right)^{-1} \quad \text{(S44)}$$

$$\tau_{LH}(E) = \beta\left(\tau_{AC,LH}^{-1}(E) + \tau_{II,LH}^{-1}(E) + \tau_{POP,LH}^{-1}(E) + \tau_{NI,LH}^{-1}(E)\right)^{-1} \quad \text{(S45)}$$

Error Estimation

Experimental errors related to thermal conductivity, electrical conductivity, and thermopower measurements were obtained mainly from uncertainty in instrumentation and dimensions. For electrical conductivity, uncertainty related to distance measurement between two probes, width, and thickness was estimated as ±4%. For thermopower measurements, uncertainty was estimated by using the largest and lowest slope as an upper (+8%) and lower bound (-4%) from the temperature-voltage relation. Thermal conductivity (k) was obtained by using the formula $k = c\rho\alpha$, where c, ρ, and α are specific heat, mass density, and thermal diffusivity, respectively. For the density measurement, estimated uncertainty was ±3% and ±2% respectively corresponding to volume and mass measurements. For thermal diffusivity, ±3% was obtained from three consecutive measurements with the flash apparatus. Therefore, the overall uncertainty corresponding to thermal conductivity measurements was estimated to be as ±8%. Overall uncertainty of the thermoelectric figure-of-merit was then calculated using the error propagation formula shown below.

$$\frac{\Delta ZT}{ZT} = 2\frac{\Delta S}{S} + \frac{\Delta\sigma}{\sigma} + \frac{\Delta k}{k} \quad \text{(S46)}$$

References

1. Bahk, J.-H.; Bian, Z.; Shakouri, A., Electron Transport Modeling and Energy Filtering for Efficient Thermoelectric $Mg_2Si_{1-x}Sn_x$ Solid Solutions. *Phys. Rev. B: Condens. Matter Mater. Phys.* **2014,** *89*, 075204-1-075204-13.
2. Wang, S.; Mingo, N., Improved Thermoelectric Properties of $Mg_2Si_xGe_ySn_{1-x-y}$ Nanoparticle-in-Alloy Materials. *Appl. Phys. Lett.* **2009,** *94*, 203109-203109-3.
3. Yi, S.-i.; Yu, C., Modeling of Thermoelectric Properties of SiGe Alloy Nanowires and Estimation of the Best Design Parameters for High Figure-of-Merits. *J. Appl. Phys.* **2015,** *117*, 035105-1-035105-12.
4. Akasaka, M.; Iida, T.; Matsumoto, A.; Yamanaka, K.; Takanashi, Y.; Imai, T.; Hamada, N., The Thermoelectric Properties of Bulk Crystalline n- and p-Type Mg_2Si Prepared by the Vertical Bridgman Method. *J. Appl. Phys.* **2008,** *104*, 013703-1-013703-8.

5. Martin, J., Thermal Conductivity of Mg_2Si, Mg_2Ge and Mg_2Sn. *J. Phys. Chem. Solids* **1972,** *33*, 1139-1148.

6. Schneider, C. A.; Rasband, W. S.; Eliceiri, K. W., NIH Image to ImageJ: 25 Years of Image Analysis. *Nat. Methods* **2012,** *9*, 671-675.